Mon. Not. R. Astron. Soc. **384,** 1200–1206 (2007) doi:10.1111/j.1365-2966.2007.12799.x

The Crab Nebula's dynamical age as measured from its northern filamentary jet

G. C. Rudie,[1,2⋆] R. A. Fesen[2⋆] and T. Yamada[3⋆]

[1]*Department of Astrophysics, MC 105-24, Caltech, 1200 E. California Blvd., Pasadena, CA 91125, USA*
[2]*Department of Physics and Astronomy, 6127 Wilder Laboratory, Dartmouth College, Hanover, NH 03755, USA*
[3]*Astronomical Institute, Tohoku University, Aoba-ku, Sendai 980-8578, JAPAN*

Accepted 2007 November 28. Received 2007 November 25; in original form 2007 August 29

ABSTRACT

We present a deep [O III] λλ4959,5007 image of the northern filamentary jet in the Crab Nebula taken with the 8.2-m Subaru telescope. Using this image and an image taken with the Kitt Peak National Observatory (KPNO) 4-m in 1988, we have computed proper motions for 35 locations in the jet. The results suggest that when compared to the main body of the remnant, the jet experienced less outward acceleration from the central pulsar's rapidly expanding synchrotron nebula. The jet's apparent expansion rate yields an undecelerated explosion date for the Crab Nebula of 1055 ± 24 CE, a date much closer to the appearance of the historic 1054 CE guest star than the 1120–1140 CE dates estimated in previous studies using filaments located within the remnant's main nebula. Our proper motion measurements suggest the jet likely formed during the 1054 supernova explosion and represents the remnant's highest velocity knots possibly associated with a suspected N–S bipolar outflow from the supernova explosion.

Key words: supernova remnants.

1 INTRODUCTION

The first object in Messier's catalogue of nebulous sources, the Crab Nebula (M1), is a young Galactic supernova remnant (SNR) and one of the most well-known astronomical objects. It possesses a variety of remarkable properties and structures including: a highly complex structure of optically bright filaments as seen in recent high-resolution *Hubble Space Telescope* images (Hester et al. 1996; Loll et al. 2004), an unusually luminous central pulsar (see Harnden & Seward 1984; Rots, Jahoda & Lyne 2004 and references therein) with accompanying X-ray jets (Brinkmann, Aschenbach & Langmeier 1985), and a radio and optically bright synchrotron nebula which exhibits fine-scale structural changes on time-scales of just days or weeks (Scargle 1969, 1970; Hester et al. 1995).

The Crab Nebula is generally considered the archetype of a pulsar driven synchrotron wind nebula (PWN) and of the so-called 'plerionic' remnants in general (see review by Davidson & Fesen 1985). The spinning magnetic field of the pulsar and strong relativistic wind of particles off the neutron star have measurably accelerated the remnant's optical filaments such that their velocities, when projected back, give a date of ∼1130 CE (Trimble 1970; Nugent 1998). This date is ∼80 yr more recent than the 1054 CE date, the year a 'guest star' associated with the Crab supernova is reported to have been observed by the Chinese and other cultures in several ancient astronomical texts (Clark & Stephenson 1977; Stephenson & Green 2002). This apparent filament acceleration, confirmed by several independent proper motion studies (see Table 1), due to an outward pressure contained within the remnant's rapidly expanding PWN is described in detail by Trimble & Rees (1970).

A particularly intriguing feature of the Crab is a faint, northern filamentary 'chimney' or 'jet' of emission filaments, which we will henceforth refer to simply as the 'jet', but which should not to be confused with the physically smaller X-ray synchrotron jets off the central pulsar. First detected in the optical by van den Bergh (1970), this optical filamentary jet consists of line-emitting filaments, especially prominent in [O III] λλ4959,5007 (Chevalier & Gull 1975). Although primarily a line-emission feature, very weak coincident non-thermal continuum emission was subsequently discovered, first in the radio (Velusamy 1984) and then in the optical (Woltjer & Véron-Cetty 1987), suggesting the jet itself is also filled with relativistic particles off the pulsar.

One especially puzzling aspect of the jet is its morphology. The first deep [O III] images of the jet showed it to be a complex network of filaments that appear to be cylindrically symmetric, but with a central axis unaligned with either the Crab's centre of expansion or pulsar (Gull & Fesen 1982). Follow-up imaging and kinematic studies (Shull et al. 1984; Véron-Cetty, Véron & Woltjer 1985; Marcelin et al. 1990) lead to several proposed explanations including a mass-loss trail from a red giant progenitor (Blandford 1983), interaction of ejecta with an interstellar cloud (Morrison & Roberts 1985) and transverse synchrotron driven shocks (Sankrit & Hester 1997). However, preliminary proper motion studies of the jet

⋆E-mail: gwen@astro.caltech.edu (GCR); fesen@snr.dartmouth.edu (RAF); yamada@astr.tohoku.ac.jp (TY)

Table 1. Results from previous proper motion studies.

Reference	Number of knots	Image epochs	Convergence date	σ (yr)
Duncan 1939	20	1909, 1938	1172	...
Trimble 1968	132	1939, 1950, 1953, 1964, 1966, 1966	1140	15
Nugent 1998	50	1939, 1960, 1976, 1992	1130	16

indicated ordinary radial motions away from the centre of expansion (Fesen & Gull 1986; Fesen & Staker 1993).

Due to the jet's greater distance from the pulsar and the remnant's synchrotron nebula, the jet may have experienced much less acceleration than most other regions of the remnant. In that case, the jet might lead to a dynamically greater remnant age leading to a date closer to the 1054 CE historic supernova sighting.

Here, we present a deep and high-resolution [O III] image of the Crab jet taken with the 8.2-m Subaru telescope. This image shows a network of extremely fine and detailed filaments. We have compared this image to a 1988 epoch image obtained with the KPNO 4-m telescope (Fesen & Staker 1993) to obtain improved proper motion measurements of its optical filaments and an estimate of the jet's expansion age.

2 OBSERVATIONS AND ANALYSIS

Optical images of the Crab Nebula were obtained 2005 October 10 using the 8.2-m Subaru telescope located on Mauna Kea. The image was taken using the Suprime-Cam Prime Focus Camera (Miyazaki et al. 2002) with the 'NB497' narrow-band filter (Hayashino et al. 2004) centred at approximately 4977 Å [full width at half-maximum (FWHM) of 77 Å]. A series of 180 s exposures taken under good seeing conditions (FWHM = 0.8 arcsec) were assembled to form a mosaic image of the entire Crab Nebula with a combined exposure time of 900 s. Fig. 1 shows the full mosaic of the Crab with Fig. 2 showing an enlarged section of the image centred on the northern jet feature.

We compared this Subaru 2005 image to a similar [O III] image taken on 1988 November 10 obtained using the KPNO Mayall 4-m telescope. The 1988 image is the same as one previously used by Fesen & Staker (1993) to estimate the proper motions of the jet. Here, we chose 35 emission knots within the upper portion of the jet (see Fig. 3) well detected on both images for proper motion measurement. The 2005 Subaru data were reduced using the Suprime-Cam Deep field Reduction package which includes bias subtraction, flat-fielding, distortion and atmospheric dispersion correction, and sky subtraction (Yagi et al. 2002; Ouchi et al. 2004). The 1988 image was reduced using standard IRAF[1] image reduction routines including bias subtraction, flat-fielding and cosmic ray rejection.

World Coordinate System (WCS) information was applied to the images in a two step process. First, stellar positions from the full 2005 image were compared with the The United States Naval Observatory (USNO) B1.0 Star Catalogue yielding a total of 232 matched fiducial stars. The rms deviation in the fit was 0.2 arcsec in both RA and Dec.

[1] The Image Analysis and Reduction Facility is distributed by the National Optical Astronomy Observatories, which are operated by the Association of Universities for Research in Astronomy, Inc., under cooperative agreement with the National Science Foundation.

The WCS fit for the 1988 image was determined in a slightly different manner. The 1988 jet image did not include the main body of the Crab and is slightly less deep than the 2005 image. Consequently, the total possible number of USNO fiducial stars in the 1988 imaged field is considerably fewer than on the Subaru image. For this reason, we correlated the 2005 imaged stellar field with the smaller 1988 image. The IRAF task 'starfind' was used to determine the WCS positions of stars in the jet region in the 2005 image. Then, from these positions, eight stars were selected due to their low proper motions and point spread functions. These stars then were used as the fiducial ties between the 2005 WCS data and the 1988 WCS image. The resulting rms deviation between the WCS fits of the 2005 and 1988 images was 0.1 arcsec in RA and Dec., and we believe the total error in the WCS matching of the two images to be less than 0.2 arcsec.

Both images were projected on to tangent planes, with proper motions computed from the corrected WCS coordinates. Knot and filament positions in the jet were visually centroided on the 1988 and 2005 images. Features were selected based mainly on the ease with which they could be reliably centroided and because they exhibited negligible shape and brightness variations apparent over the 17.1 yr time interval between the two images.

The absolute accuracy of our proper motion measurements was limited by the lower resolution of the 1988 image (FWHM = 1.0 arcsec) and by the often diffuse nature of the knots and filaments. We estimate the errors of our centroided jet knot positions to be generally better than 0.3 arcsec on the 1988 image and 0.2 arcsec on the 2005 image. The resulting proper motion estimates should be more reliable and accurate than the prior study of Fesen & Staker (1993) of the jet principally due to the deeper and higher resolution of the 2005 jet image and a longer time interval (17 yr) between images (Fesen & Gull 1986; Fesen & Staker 1993).

3 RESULTS

Our primary goal was to investigate whether the jet's knots and filaments experienced less acceleration due to their greater distance from the Crab pulsar and its rapidly expanding synchrotron nebula. In order to test and verify the accuracy of our measurement technique for the jet knots and filaments, we also included measurements for several emission knots in the bright, inner portion of the remnant studied by Trimble (1968) and Nugent (1998). For these knots, we made measurements on the 2005 Subaru image and also an image taken on 1959 November 28 by N. Mayall with the 120-inch Lick Telescope.

Proper motion measurements were computed for a total of 140 knot and filament positions distributed throughout the main nebula and the northern jet. Measurements for knots located within the main body of the remnant resulted in proper motion estimates ranging between 0.04 and 0.21 arcsec yr^{-1} corresponding to transverse velocities of 350–1820 km s^{-1} at a distance of 1.83 kpc (Davidson & Fesen 1985). Looking only at those knots measured in previous studies, projected-back motions yielded estimated explosion dates

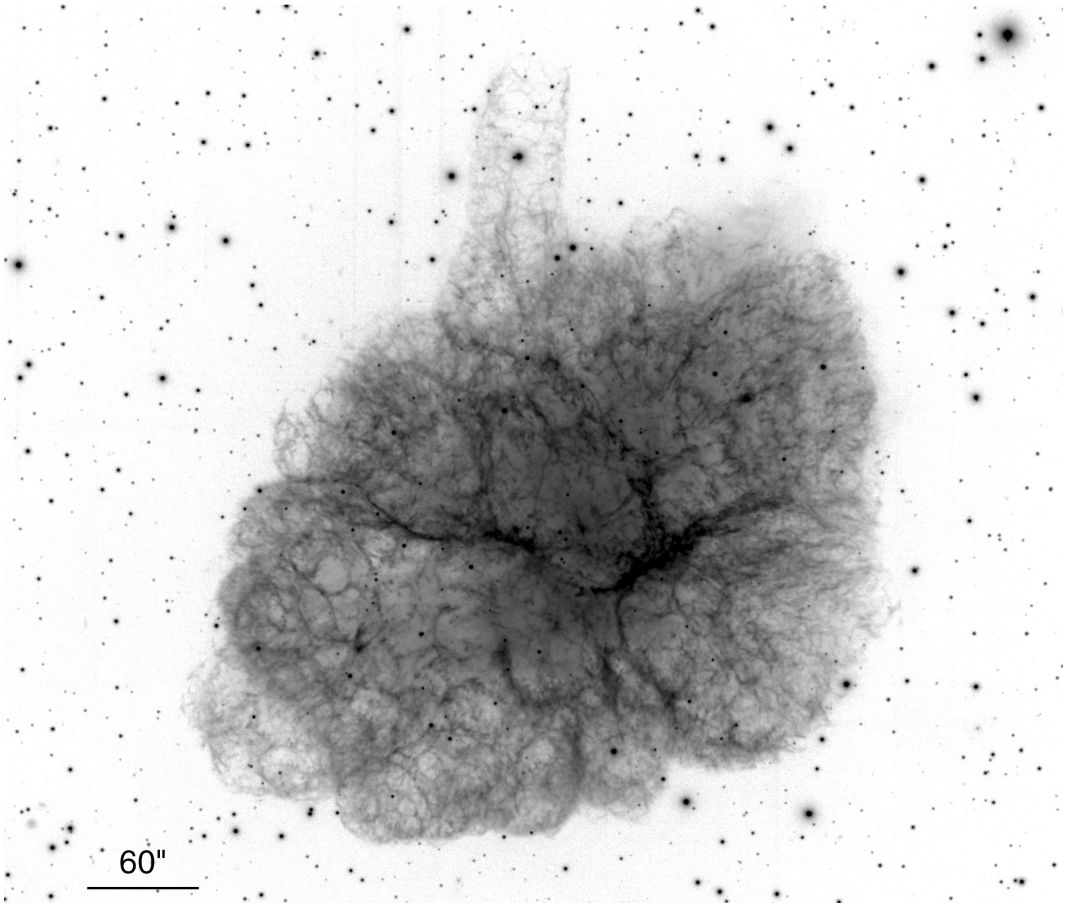

Figure 1. Subaru [O III] image of the Crab Nebula using a log intensity stretch to show the position of the northern filamentary jet in relation to the remnant's brighter inner filament complex.

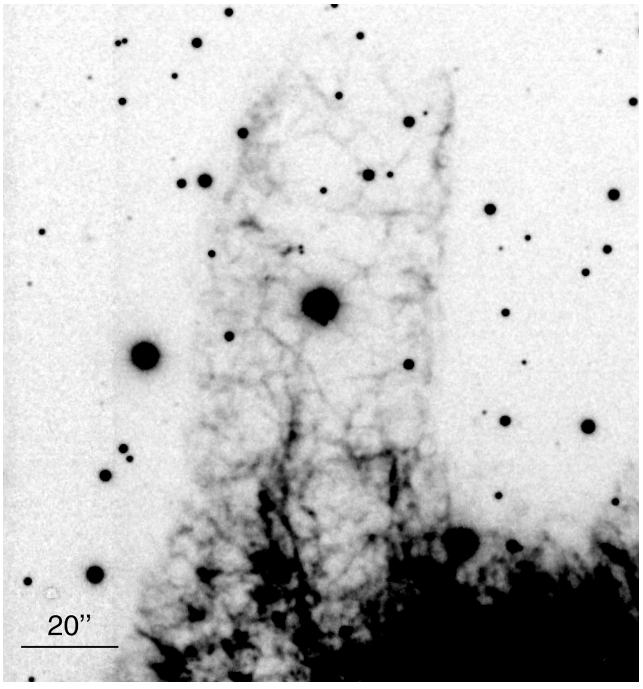

Figure 2. An enlarged section of the 2005 Subaru [O III] image of the Crab Nebula showing its northern jet.

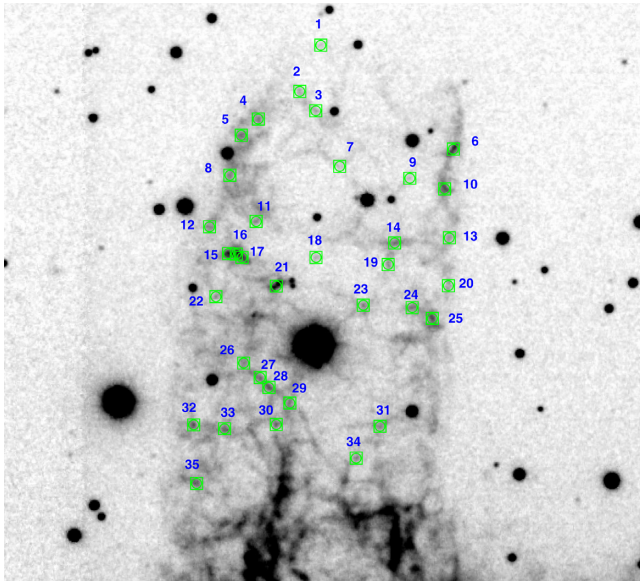

Figure 3. Subaru [O III] image of the northern jet with the 2005 positions of the 35 measured jet ejecta knots marked.

of 1136 CE for 23 of Nugent's knots and 1146 CE for 42 of Trimble's knots, consistent with their reported convergence dates of 1130 and 1140 CE, respectively (Trimble 1968; Nugent 1998).

Measurements of 35 knots located in the northern half of the jet (see Fig. 3) give a range of proper motion estimates of 0.19–0.29 arcsec yr^{-1}, corresponding to a transverse velocity range of 1650–2520 km s^{-1} at a distance of 1.83 kpc (Davidson & Fesen 1985). We also examined the motion of each individual knot and projected their positions back into the nebula. For each of these knots, we obtained an estimated convergence date back to the remnant's centre. We chose the remnant's centre of expansion as estimated by Nugent (1998) and derived the convergence date as the year when the knot's backward motion was closest to this expansion point. The resulting convergence dates are listed in Table 2. The average of these dates suggests an explosion date of 1050 CE with a standard deviation of 27.5 yr.

Differences in the positional measurement uncertainties for the 35 jet knots selected lead to several knots missing the expansion point by larger values than the average of the sample. Therefore, in order to try to improve our convergence date, we selected a smaller knot sample which included just those knots which showed the most radial proper motions, i.e., motions which when projected back fell within 10 arcsec of the Nugent (1998) centre of expansion. Out of the 35 knots measured in the top of the jet, 22 had proper motions which projected within this radius. This knot sample gave an average convergence date of 1055 CE with a standard deviation of 24 yr. Fig. 4 shows the scatter in the date given by all 34 measured jet knots with the larger symbol (dots) indicating those which projected closest to the expansion centre.

In order to help judge the meaning of these northern jet proper motion results, proper motion estimates were also made from the same images for knots in the southernmost part of the jet and outside of the jet to the east and west, along the northernmost periphery of the Crab's optical structure. The results of these measurements are listed in Table 3. These knot measurements yielded convergence dates considerably earlier than those obtained from knots located in the main part of the remnant but still later than the date we derived from the northernmost jet knots. Specifically, the 17 measured knots located in the base of the jet whose projected-back proper motions fall within 10 arcsec of the centre of expansion give a convergence

Table 2. Proper motion measurements for jet knots.

Knot ID	Convergence[a] Date	D_{CE}[b] (arcsec)	μ_x (arcsec yr^{-1})	μ_y (arcsec yr^{-1})	μ_T (arcsec yr^{-1})	α (J2000)[c] (h m s)	δ (J2000)[c] (° arcmin arcsec)
1	1095	7.276	0.02	0.29	0.29	05 34 33.692	+22 05 13.98
2	1066	4.404	0.01	0.27	0.28	05 34 33.971	+22 05 05.45
3	1092	11.639	0.03	0.28	0.28	05 34 33.759	+22 05 01.88
4	1065	1.344	0.03	0.27	0.27	05 34 34.523	+22 05 00.36
5	1090	12.195	0.04	0.27	0.27	05 34 34.749	+22 04 57.36
6	1054	9.951	−0.02	0.26	0.26	05 34 31.929	+22 04 54.81
7	1059	3.076	0.01	0.26	0.26	05 34 33.440	+22 04 51.64
8	1015	15.081	0.05	0.24	0.25	05 34 34.901	+22 04 49.99
9	1035	2.589	−0.01	0.25	0.25	05 34 32.508	+22 04 49.44
10	1044	6.287	−0.02	0.25	0.25	05 34 32.045	+22 04 47.47
11	1048	7.347	0.03	0.24	0.25	05 34 34.552	+22 04 41.48
12	1067	4.962	0.04	0.25	0.25	05 34 35.171	+22 04 40.49
13	1039	14.228	−0.03	0.24	0.24	05 34 31.983	+22 04 38.45
14	1050	7.636	−0.01	0.24	0.24	05 34 32.709	+22 04 37.49
15	1023	9.589	0.04	0.23	0.23	05 34 34.918	+22 04 35.54
16	1001	10.281	0.04	0.22	0.23	05 34 34.816	+22 04 35.45
17	1029	11.021	0.04	0.23	0.23	05 34 34.740	+22 04 34.83
18	1028	9.539	0.02	0.23	0.23	05 34 33.755	+22 04 34.83
19	1004	11.673	−0.01	0.22	0.23	05 34 32.796	+22 04 33.51
20	1038	13.634	−0.02	0.23	0.23	05 34 31.995	+22 04 29.60
21	1083	6.839	0.03	0.24	0.24	05 34 34.285	+22 04 29.55
22	1085	10.776	0.05	0.24	0.24	05 34 35.086	+22 04 27.58
23	1087	4.165	0.00	0.24	0.24	05 34 33.127	+22 04 26.01
24	1011	3.100	−0.01	0.22	0.22	05 34 32.477	+22 04 25.57
25	1020	18.716	−0.03	0.22	0.22	05 34 32.209	+22 04 23.55
26	1081	5.428	0.04	0.22	0.23	05 34 34.716	+22 04 15.33
27	1024	12.762	0.01	0.21	0.21	05 34 34.498	+22 04 12.67
28	1028	11.971	0.01	0.21	0.21	05 34 34.381	+22 04 10.86
29	1051	8.362	0.01	0.21	0.21	05 34 34.103	+22 04 07.95
30	1055	1.637	0.02	0.21	0.21	05 34 34.284	+22 04 04.00
31	1076	6.288	0.05	0.21	0.21	05 34 35.381	+22 04 03.93
32	1063	4.861	−0.00	0.21	0.21	05 34 32.904	+22 04 03.66
33	1067	7.809	0.04	0.21	0.21	05 34 34.972	+22 04 03.23
34	1007	0.479	0.01	0.19	0.19	05 34 33.222	+22 03 57.80
35	1066	11.303	0.05	0.19	0.20	05 34 35.343	+22 03 53.13

[a]Estimated date of knot's closest (least-squared distance) to the centre of expansion.
[b]The projected shortest distance between the knot and the centre of expansion.
[c]Knot J2000 coordinates on the 2005 Subaru image.

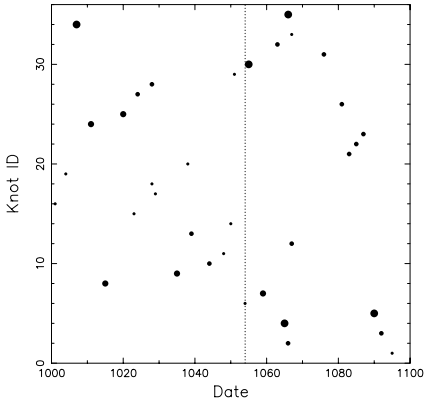

Figure 4. Plot of the computed convergence date of each knot upon the centre of expansion. The size of the dot in the figure corresponds inversely to the distance between the traced-back motion of the knot and the centre of expansion. Thus, the largest dots correspond to those knots which project back closest to the centre of expansion.

date of 1081 ± 37 yr. The 22 measured knots located to the east and west of the jet's base whose projected-back proper motions also fall within 10 arcsec of the centre of expansion give a convergence date of 1077 ± 45 yr.

In Fig. 5, we show the projected motions of all 35 northern jet knots for an expansion date of 1055 CE, both for our measured knot proper motion paths (right-hand side figure), and then assuming the motions of the knots were completely radial, tracing perfectly away from the centre of expansion as defined by Nugent (1998) (left-hand side figure). Overall, the observed motions of knots within the jet region suggest a nearly radial expansion and trace back to a location very close to the remnant's nominal centre of expansion. Our estimated positional measurement errors could have resulted in up to a 3° change in direction which would account for a substantial fraction of the apparent non-radial motions seen in the right-hand side figure. Thus, despite the jet's strongly overall non-radial appearance with its long axis misaligned with the remnant's centre, individual jet knots and filaments appear to move in a radial fashion away from the remnant's estimated explosion centre.

Two additional things should be noted from Fig. 5. The first is that a substantial number of jet knots appear to cross at a position north of the centre of expansion. Secondly, knots located along the jet's western limb tend to show a convergence point east of the centre of expansion, while knots along the jet's eastern side appear to favour a convergence point west of the centre of expansion. Both these effects might indicate a small, non-radial component to the jet's expansion which will be addressed below.

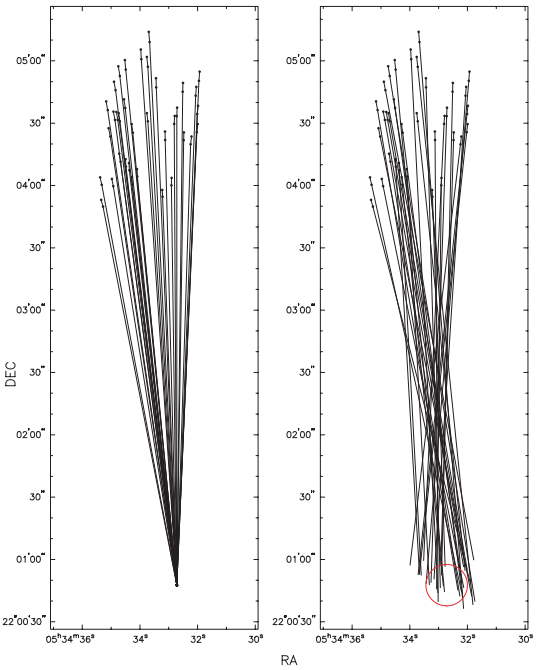

Figure 5. Plots of the extrapolated proper motions of the jet knots. Both plots show two points, the measured positions of the knots in 2005 and 1988. The lines in the left-hand side plot show what the motions would look like if they were perfectly radial. The lines in the right-hand side plot show the true measured motions of the knots. The red circle is 10 arcsec in radius centred on the centre of expansion.

4 DISCUSSION

4.1 Dynamical age of the Crab Nebula

Our computed convergence date for the jet is 1055 ± 24 CE, in excellent agreement with historical records which indicate the Crab SN occurred in the year 1054. We attribute the reason for the difference between our result and earlier age estimates to be chiefly the jet's northernmost knots experiencing little appreciable acceleration by the pulsar's rapidly expanding synchrotron nebula. All previous age estimates based upon proper motion studies used knots and filaments located within the main body of the Crab remnant. Consequently, interior knot motions reflected both an expansion due to the SN event itself and a post-SN acceleration resulting from the interaction of the pulsar wind nebula. Although the 1054 explosion date for the Crab Nebula's SN has not been in serious doubt, it is none the less valuable to have a direct confirmation based on expansion dynamics.

Table 3. Summary of proper motion measurements.

Region	r range (arcsec)	Number of knots[a]	Image epochs	μ_T (arcsec yr^{-1})	Convergence date	σ (yr)
Top of jet	190–270	22	1988.7–2005.8	0.19–0.29	1055	24
Base of jet	120–160	17	1988.7–2005.8	0.14–0.17	1081	37
SE and SW of jet base	110–180	22	1988.7–2005.8	0.11–0.19	1077	45
Whole SNR, Nugent	60–180	23	1960.7–2005.8	0.06–0.20	1136	68
Whole SNR, Trimble[b]	40–180	42	1960.7–2005.8	0.04–0.21	1146	54

[a]The number of knots quoted here reflects the number of knots whose projected-back proper motions fell within 10 arcsec of the centre of expansion.
[b]Trimble's filament proper motions computed adopting Nugent's centre of expansion.

Although the jet's knots and filaments appear not to have been significantly accelerated radially away from the remnant's central region, our measured jet knot proper motions may indicate a small, non-radial component. As shown in Fig. 5 (right-hand panel), the projected motions of the knots intersect north of the position of the centre of expansion. This effect may not represent the actual nature of the jet as there are several sources of error which could contribute to this motion. First, it is possible that there may be a slight rotational shift between the two World Coordinate System fits for the images. Because the original motions of the jet ejecta were so close to directly northward, a slight shift east or west would cause a much more notable change in the E–W component of their proper motion than would a similarly sized shift in the N–S direction. Thus, the directions of the knots would be greatly affected by such a shift, while the velocities would show considerably less error. Secondly, an error in centroiding the knots can account for a slight shift as well. Our computed errors show a change in direction of approximately 3° is possible which could account for the non-radial motions of the knots.

On the other hand, it is possible that the measured motions do reflect the jet's true expansion properties. The jet is essentially a hollow structure and as shown by Velusamy (1984) and Woltjer & Véron-Cetty (1987), the jet does contain some faint synchrotron emission, most visible at its southern base. If this plasma induced an acceleration that was largely against the jet's filamentary walls, this might act to expand the jet in the E–W plane and explain why the north-western jet knots end up east of the centre of expansion while most knots located at the north-eastern portion of the jet project back west of the centre of expansion. Since our derived expansion date for the jet is most sensitive to N–S motions, such an acceleration would not significantly effect our estimated dynamical age.

4.2 The nature of the jet

Our proper motion measurements provide a valuable constraint on the origin of the Crab's northern jet of ejecta. A successful jet formation model should explain the jet's non-radial appearance, its peak expansion velocity, specific location along the remnant's outer periphery and the lack of any obvious counter-jet to the south. Below, we briefly review some of the proposed theories for the jet's origin and discuss them in relation to our dynamical measurement results.

4.2.1 Plasma instabilities models

Several authors have suggested the jet is a post-SN feature resulting from an interaction between the ejecta and the pulsar wind nebula. Many variations of plasma instability models have been suggested including: (i) an aneurysm of ejecta pushed aside by the pulsar's plasma flow (Bychkov 1975; Véron-Cetty et al. 1985; Marcelin et al. 1990), (ii) Rayleigh–Taylor instabilities (Chevalier & Gull 1975; Kundt 1983) or differential acceleration (Chevalier & Gull 1975), (iii) pressure from swept-up magnetic field lines (Shull et al. 1984), (iv) ejecta entrainment in magnetic fields formed by highly ordered outflows from the polar caps of the pulsar itself (Benford 1984) and (v) synchrotron driven shocks (Sankrit & Hester 1997).

A particularly attractive feature of such models is their ability to explain both the non-radial appearance of the jet and the lack of a counter-jet to the south. However, our proper motion measurements indicate an essentially radial expanding jet. Moreover, some of these plasma instability models call for greater acceleration of the jet's filaments than those found in the main body of the nebula (Chevalier & Gull 1975; Shull et al. 1984), or a younger age compared to the rest of the nebula (Kundt 1983). While a greater degree of acceleration or a younger age for the jet is not supported by our data which suggests a current jet age around 950 yr similar to the Crab's historic age, a more modest expansion breakout acceleration is not completely ruled out by our proper motion measurements.

For most plasma instability ('blowout') models, the exact location of a high-velocity 'jet' along the remnant's outer boundary is undefined but with a greater likelihood along the pulsar's NW–SE wind injection axis. However, the remnant's filamentary jet is some 45° away from the pulsar's synchrotron jets, which lie along a NW–SE axis (PA $= 300^\circ$; Ng & Romani 2004). Along this NW–SE axis, the PWN appears to have pushed aside the remnant's outer ejecta filaments creating a virtual hole in the filamentary ejecta along the NW limb (Lawrence et al. 1995; Čadež, Carremiãna & Vidrih 2004). There the synchrotron emission can be seen to leak out of the remnant's thick thermal plasma shell in optical, X-rays and radio images of the remnant. The lack of extended filamentary line-emission ejecta in this region similar to the northern 'jet' is suggestive that the northern jet was not the result of a breakout of the pulsar's synchrotron wind nebula.

4.2.2 An asymmetrical explosion?

Despite a lack of an obvious southern counter-jet, the remnant's northern jet might represent high-velocity ejecta resulting from a N–S bipolar expansion asymmetry. In 1989, MacAlpine et al. showed that N–S oriented spectral drift scans of the Crab revealed a nearly N–S bipolar structure. The data showed that the pinched waist of the hourglass-like expansion coincided with a band of helium rich filaments (a 'high-helium band') in which the computed helium mass fraction was at least 75 per cent (Uomoto & MacAlpine 1987). MacAlpine et al. (1989) suggested a helium rich circumstellar torus or disc could have resulted in constrained velocities in the horizontal region around the progenitor. Subsequent drift scans of the remnant by Fesen, Shull & Hurford (1997) and Smith (2003) confirmed the presence of a strong bipolar expansion.

Additional support for a circumstellar torus was presented by Schmidt, Angel & Beaver (1979) and Fesen, Martin & Shull (1992) who examined the east and west indentations seen in the synchrotron emission (the synchrotron bays), and suggested these may have be caused by an E–W magnetic torus associated with the E–W band of He-rich filaments. Such a magnetic torus might constrain the E–W expansion of the PWN, leaving the bay indentations seen today.

In an asymmetrical explosion model for the jet, its location along the northern edge of the remnant is not accidental (Fesen & Staker 1993). The alignment of the jet with the northern extent of the north expansion bubble seen in spectral drift scans of the remnant plus its major axis aligned nearly perpendicular to the synchrotron bays suggest a causal link between the jet and a possible constrained E–W expansion of the SN ejecta. The lack of an equally obvious southern 'counter-jet' might be explained by either a weaker ejection of material to the south and/or increased ejecta confinement, and indeed drift scans of the remnant do show higher velocities to the north compared to the south, relative to the pinched central zone (MacAlpine et al. 1989; Fesen et al. 1997; Smith 2003).

The jet's filaments, being farther from the pulsar's energetic wind, would experience less acceleration compared to knots and filaments located in the main body of the nebula. Our measurements of other locations at the base of the jet and to the east and west appear

consistent with this picture, showing larger dynamical ages correlating with their increased distance from the pulsar (see Table 3).

Finally, we note that our computed expansion age of the jet, although yielding an expansion age consistent with the historic SN sighting in the year 1054, could also be viewed consistent with an initial acceleration by the pulsar and subsequent deceleration through an interaction with a suspected outer halo of unshocked ejecta (Chevalier 1977; Murdin & Clark 1981; Lundqvist, Fransson & Chevalier 1986; Hester et al. 1996). The presence of appreciable outer ejecta, however, remains highly controversial with several radio, optical and X-ray observations failing to find any supportive evidence for its existence (Frail et al. 1995; Fesen, Shull & Hurford 1997; Wallace et al. 1999; Seward, Gorenstein & Smith 2006). In any case, we view it as unlikely that the degree of any PWN acceleration and possible outer ejecta induced deceleration would be so nearly offsetting as to lead to the currently derived jet expansion date of around CE 1054.

5 SUMMARY

Proper motion analysis of 35 ejecta knots in the northern filamentary jet in the Crab Nebula shows the ejecta which form the jet to be less accelerated than the main body of the nebula. Traced-back proper motions give an explosion date of 1055 $\pm$ 24 CE which lie in much closer agreement to the appearance of the 1054 CE historical guest star. The measured proper motions are largely radial and directed away from the centre of expansion. These data suggest the jet was likely formed in the original explosion possibly as a result of bipolar SN kinematics in which the E–W expansion of the ejecta was constrained by the presence of a circumstellar disc.

ACKNOWLEDGMENTS

This research was partially funded by a DOF Research Grant, the ORL SS program and the Richter Memorial fund from Dartmouth College. We thank Molly Hammell for considerable programming assistance and Yuki Nakamura for reduction of the Suprime Cam image. This work is based in part on data collected at Subaru Telescope, which is operated by the National Astronomical Observatory of Japan.

REFERENCES

Benford G., 1984, ApJ, 282, 154
Blandford R. D., Kennel C. F., McKee C. F., Ostriker J. P., 1983, Nat, 301, 586
Brinkmann W., Aschenbach B., Langmeier A., 1985, Nat, 313, 662
Bychkov K. V., 1975, Soviet Astronomy. AJ, 18, 420
Čadež A., Carremiãna A., Vidrih S., 2004, ApJ, 609, 797
Chevalier R. A., 1977, in Schramm D. N., ed., Supernovae. Reidel, Dordrecht, p. 53
Chevalier R. A., Gull T. R., 1975, ApJ, 200, 399
Clark D. H., Stephenson F. R., 1977, The Historical Supernovae. Oxford, Pergamon
Davidson K., Fesen R. A., 1985, ARA&A, 23, 119
Fesen R. A., Gull T. R., 1986, ApJ, 306, 259
Fesen R. A., Staker B., 1993, MNRAS, 263, 69
Fesen R. A., Martin C. L., Shull J. M., 1992, ApJ, 399, 599
Fesen R. A., Shull J. M., Hurford A. P., 1997, AJ, 113, 354
Frail D. A., Kassim N. E., Cornwell T. J., Goss W. M., 1995, ApJ, 454, L129
Gull T. R., Fesen R. A., 1982, ApJ, 260, L75
Harnden F. R. Jr., Seward F. D., 1984, ApJ, 283, 279
Hayashino T. et al., 2004, AJ, 128, 2073
Hester J. J. et al., 1995, ApJ, 448, 240
Hester J. J. et al., 1996, ApJ, 456, 225
Kundt W., 1983, A&A, 121, L15
Lawrence S. S., MacAlpine G. M., Uomoto A., Woodgate B. E., Brown L. W., Oliversen R. J., Lowenthal J. D., Liu C., 1995, AJ, 109, 2635
Loll A., Hester J. J., Sankrit R., Blair W., 2004, BAAS, 36, 1521
Lundqvist P., Fransson C., Chevalier R. A., 1986, A&A, 162, L6
MacAlpine G. M., McGaugh S. S., Mazzarella J. M., Uomoto A., 1989, ApJ, 342, 364
Marcelin M., Veron-Cetty M. P., Woltjer L., Boulesteix J., D'Odorico S., Lecoarer E., 1990, A&A, 228, 471
Miyazaki S. et al., 2002, PASJ, 54, 833
Morrison P., Roberts D., 1985, Nat, 313, 661
Murdin P., Clark D. H., 1981, Nat, 294, 543
Ng C.-Y., Romani R. W., 2004, ApJ, 601, 479
Nugent R. L., 1998, PASP, 110, 831
Ouchi M. et al., 2004, ApJ, 611, 660
Rots A. H., Jahoda K., Lyne A. G., 2004, ApJ, 605, L129
Sankrit R., Hester J. J., 1997, ApJ, 491, 796
Scargle J. D., 1969, ApJ, 156, 401
Scargle J. D., 1970, PASP, 82, 388
Schmidt G. D., Angel J. R. P., Beaver E. A., 1979, ApJ, 227, 106
Seward F. D., Gorenstein P., Smith R. K., 2006, ApJ, 636, 873
Shull P., Carsenty U., Sarcander M., Neckel T., 1984, ApJ, 285, L75
Smith N., 2003, MNRAS, 346, 885
Stephenson F. R., Green D. A., 2002, Historical Supernovae and their Remnants. Claredon Press, Oxford, p. 117
Trimble V., 1968, AJ, 73, 535
Trimble V., 1970, PASP, 82, 375
Trimble V., Rees M., 1970, Astrophys. Lett., 5, 93
van den Bergh S., 1970, ApJ, 160, L27
Velusamy T., 1984, Nat, 308, 251
Véron-Cetty M. P., Véron P., Woltjer L., 1985, A&A, 151, 101
Wallace B. J., Landecker T. L., Kalberla P. M. W., Taylor A. R., 1999, ApJS, 124, 181
Woltjer L., Véron-Cetty M.-P., 1987, A&A, 172, L7
Uomoto A., MacAlpine G. M., 1987, AJ, 93, 1511
Yagi M., Kashikawa N., Sekiguchi M., Doi M., Yasuda N., Shimasaku K., Okumura S., 2002, AJ, 123, 66

This paper has been typeset from a TEX/LATEX file prepared by the author.